SANDIA REPORT
SAND2001-0698
Unlimited Release
Printed March 2001

EBW Gapping Study

Kenneth C. Chen and William P. Brigham

Prepared by
Sandia National Laboratories
Albuquerque, New Mexico 87185 and Livermore, California 94550

Sandia is a multiprogram laboratory operated by Sandia Corporation, a Lockheed Martin Company, for the United States Department of Energy under Contract DE-AC04-94AL85000.

Sandia National Laboratories

Issued by Sandia National Laboratories, operated for the United States Department of Energy by Sandia Corporation.

Available to DOE and DOE contractors from
U.S. Department of Energy
Office of Scientific and Technical Information
P.O. Box 62
Oak Ridge, TN 37831

Telephone: (865)576-8401
Facsimile: (865)576-5728
E-Mail: reports@adonis.osti.gov
Online ordering: http://www.doe.gov/bridge

Available to the public from
U.S. Department of Commerce
National Technical Information Service
5285 Port Royal Rd
Springfield, VA 22161

Telephone: (800)553-6847
Facsimile: (703)605-6900
E-Mail: orders@ntis.fedworld.gov
Online order: http://www.ntis.gov/ordering.htm

SAND2001-0698
Unlimited Release
Printed March 2001

EBW Gapping Study

Kenneth C. Chen
System Surety Assessment Department

William P. Brigham
Explosive Projects and Diagnostic Department

Sandia National Laboratories
P. O. Box 5800
Albuquerque, New Mexico 87185-0492

Abstract

This report details a study of exploding bridgewire (EBW) gapping by a DC current and reports the voltage and detonation sensitivities of the resulting gapped EBWs. The study concerns possible gapping of EBWs by unintended electrical signals and the safe handling of potentially gapped EBWs. A range of current levels commonly encountered is used to gap the EBWs. Action required for gapping is experimentally determined to be approximately equal to the bridgewire burst action. Gap lengths are experimentally determined and compared to analytical results, and voltage breakdown thresholds and detonation sensitivities are obtained. In contrast to a spark gap EBW, the electrically gapped EBWs are found to be less sensitive to detonation than normal firing. Further investigations should be made to confirm this observation.

Acknowledgement

The authors would like to thank R. S. Lee of Lawrence Livermore National Laboratory for discussions on test planning and data interpretations. The first author would also like to thank J. E. Kennedy of Los Alamos National Laboratory for stimulating discussions on spark gap detonators and L. K. Warne for enlightening discussions on gap modeling.

Contents

Figures

Tables

Introduction

Spark-gap detonators are more sensitive to electrical energy than regular exploding bridgewire (EBW) detonators. Tucker et al. studied firing properties of spark-gap detonators [1] and found that a 10-mil gap with fine PETN (10,500 cm^2/g of specific surface area, 0.88 g/cm^3 of density) could be detonated by as low as 7 mJ of capacitive discharge current[1].

In 1966, Furnberg [2] reported bridgewire gapping of Mound built SE-1 exploding bridgewires (EBWs) by current levels considerably lower than the required detonation current and considerably longer in pulse duration but with sufficient energies and actions to gap the bridgewires. An EBW can be gapped and could be sensitized by battery current (or A/C current); a subsequent voltage spike such as power line surge could initiate the detonators. Furnberg's investigation is somewhat inconclusive in that (1) the gap length cannot be related to the applied current in a consistent manner; (2) a first-principle analysis was not given; and (3) detonation evidence for firing gapped EBWs was not provided.

The purpose of this report is to systematically investigate the physics of gapping and the potential safety threat of the gapped EBWs. First, the existing empirical database on burst (complete vaporization) action for exploding bridgewire detonators [3] are used to determine time to bridgewire opening. Action is used as a parameter for test planning because it is not very sensitive to heat loss or energy loss. Second, the gapping circuit and board are discussed, and gapping data presented. An empirical relationship between gap length and current level is determined. A one-dimensional nonlinear heat equation is used to describe the gap formation by electrical pulses. The voltage breakdown threshold levels for gapped EBWs and their detonation sensitivities are also determined. Finally, the detonator under test for its detonation threshold is glued to an aluminum block. After the test, detonator detonation or deflagration can then be identified by the presence or absence of dents on aluminum blocks [4].

[1] Table 2 of Reference 1.

Overview

A typical firing set uses a firing pulse of less than 1 μs in duration. In this case, the thermal loss during the application of a firing pulse is negligible. Tucker and Toth [3] tabulated the resistivity of twenty-two common metals as a function of applied specific action ($\frac{1}{A^2}\int I^2 dt$) and applied energy density ($\frac{1}{V}\int RI^2 dt = \frac{1}{A^2}\int \rho I^2 dt$, with $\rho = 1/\sigma$), with ρ and σ being the resistivity and conductivity of the metal, respectively.

The specific actions (A^2-sec/mm^4) for different materials are given in [3]. The bridgewire burst action, defined as

$$\int_0^t I^2 dt = K_b D^2,$$

is a function of material and bridgewire diameter D in mils. When D is 1 mil, the burst action, K_b, required for a given metal can be tabulated. K_b for twelve more common metals are given in Table 1. The area used for this calculation is $0.5^2 \pi\, mil^2 = 5.0675\times10^{-4}\, mm^2$, and the square of the area is used to obtain K_b from the data given in [3].

Table 1. Burst Action Coefficients for Common Metals

Metal	Burst Action Coefficient K_b
Copper	0.044
Aluminum	0.017
Gold	0.022
Silver	0.029
Platinum	0.013
Nickel	0.014
Iron	0.009
Tungstan	0.022
Titanium	0.0049
Lead	0.0015
Zinc	0.01
Uranium	0.009

"Action" is a convenient parameter to describe the physics of bridgewire gapping because it does not account for the dynamic resistivity of the bridgewire and thus is not very sensitive to heat loss or energy loss. The tabulated action values for burst (Table 1) obtained for sub-microsecond pulses by Tucker et al. can be used to determine the time-to-opening for different current waveforms and levels for different metallic bridgewire sizes. The value for gold is used to provide preliminary test planning and post-test analysis for gapping in the sub-millisecond region (Section on Gapping Data Analysis

and Figure 18). It must be emphasized that the action for burst, not the action for melt (which is approximately one half of the action for burst) must be used for this calculation.

Experimental Plan

Test Unit

A Reynolds EBW detonator, RP-87, was used for the bridgewire gapping study. An RP-87 has a post-to-post spacing (standard bridgewire spacing) of 20 mils. A 1-mil diameter rather than the standard 1.3-mil diameter gold bridgewire (for RP-87) was used for testing. The resulting detonator has a 1-mil by 20-mil bridgewire. Ten detonators without explosive (bare bridgewire detonators) were ordered for testing; the remaining one hundred detonators were fully loaded with PETN. Detonators with bare bridgewires were used because their gaps can be captured by a microscope. Figure 1 shows the basic configuration of an RP-87. Note that the post diameter is equal to the bridgewire spacing. A microscope picture of bare bridgewire detonator is shown in Figure 2.

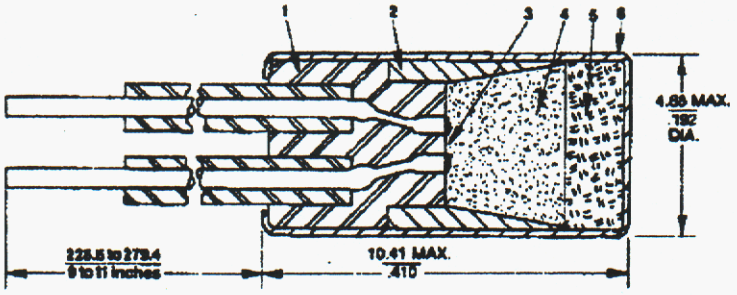

PARTS DESCRIPTION

1. PLASTIC HEADER, FM #4005 PHENOLIC
2. STEEL SLEEVE
3. GOLD BRIDGEWIRE
4. INITIATING EXPLOSIVE, 25 MG OF PETN
5. OUTPUT EXPLOSIVE, 48 MG OF RDX
6. SEAL CUP, 0.006 THICK STAINLESS STEEL

Figure 1. RP-87 detonator description.

Test Objectives

The test had several objectives as stated below:

(1) Experimentally determine bridgewire gapping by a DC current to obtain parameters controlling gap length.

(2) Study the bridgewire configurations after gapping.

(3) Experimentally assess PETN thermal loading on the bridgewire heating by comparing time to bridgewire opening for bare bridgewire and full detonators.

(4) Experimentally determine the breakdown threshold voltage for the gapped EBW.

(5) Determine the approximate detonation current level for the gapped EBW by using a witness aluminum block.

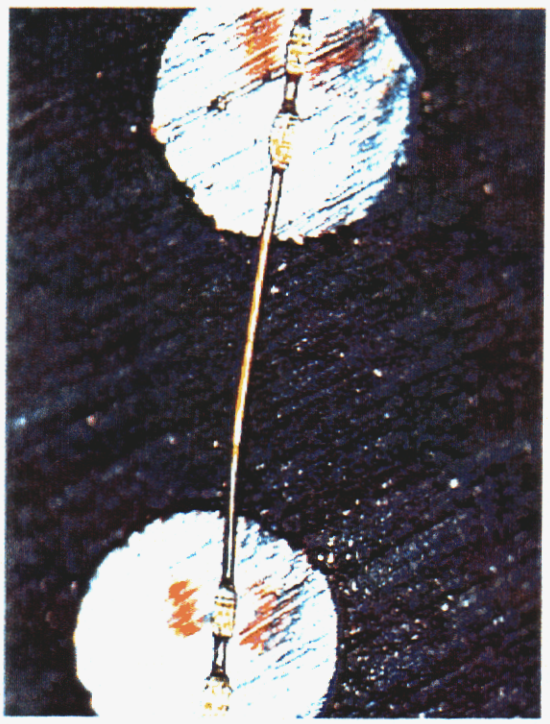

Figure 2. Microscope picture of a bare bridgewire detonator.

EBW Gapping Test Plan

Threshold current for gapping of a 1-mil by 20-mil gold bridgewire was empirically determined to be approximately 3A. Large deviations for time to bridgewire opening were expected near the threshold current. Therefore, three bare detonators were subjected to 3A; in addition, one bare bridgewire detonator was subjected to current levels of 4A, 5A, 6A, 7A and 8A. The resulting gaps were captured using a microscope.

Groups of 10 full detonators were subjected to 3A, 4A, 5A, 6A, 8A, 12A, 15A, and 20A, followed by radiography of the gaps.

Test current levels for bare bridgewire and full detonators were prescribed to cover the full range of the gap length variation. In order to obtain data for deriving the action and energy for each test, for providing some insight into the gapping process, and for assessing PETN thermal loading, current on and voltage across the detonators were monitored.

Sensitivity Testing of Resulting Gapped EBWs

All gapped, bare detonators and some gapped, full detonators were tested for their threshold breakdown voltages by using a short-time voltage tester.

Most remaining gapped, full detonators were subjected to a discharge current provided by the Sandia Cable Discharge System. The gapped detonator was glued to an aluminum witness block before firing, and the indentation depth on the block after the test was used as evidence for detonation.

EBW Gapping

EBW Gapping Experiment Setup

The gapping circuit (Figure 3) has a Hewlett Packard Harrison 6268A DC power supply (up to 40V and 30A) for V2 and a Stanford Research System Model DG635 square pulse generator was to trigger the silicon controlled rectifier (SCR). The voltage across the detonator (at positions 1 and 2) and the current on a one ohm series resistor were monitored. The SCR controls the beginning of the applied electrical stress and the bridgewire opening controls the end of the stress.

The gapping board (Figure 4) indicates that positions 1 and 2 in the circuit (Figure 2) were tapped off by clipping leads to the voltage probe. (The differential voltage probe circuit used for voltage measurement can be found in Reference [5]). The gold-colored circuit element to the right of clip leads is the one ohm resistor; the gray circular ring disk is the SCR; and the red and blue cube is the isolation transformer.

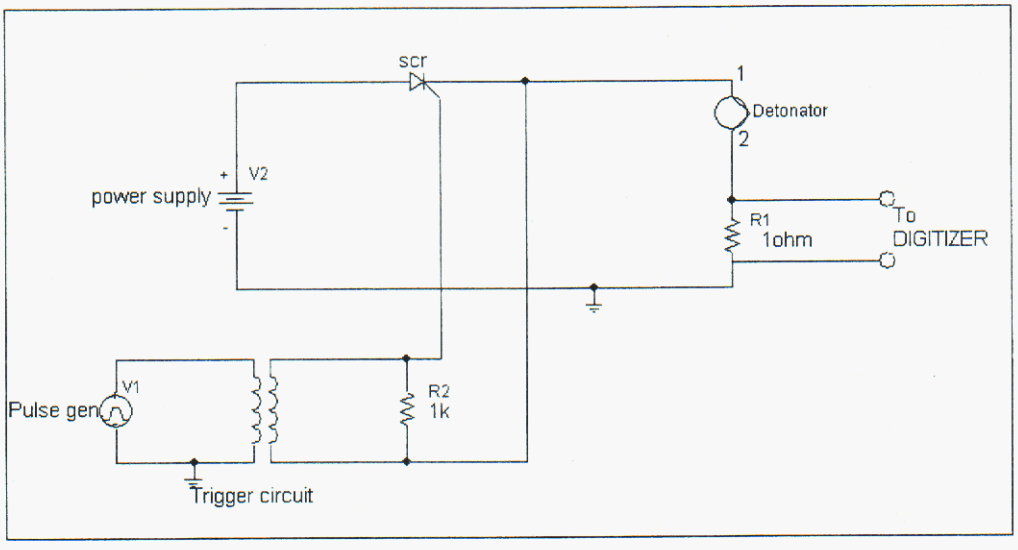

Figure 3. Gapping circuit.

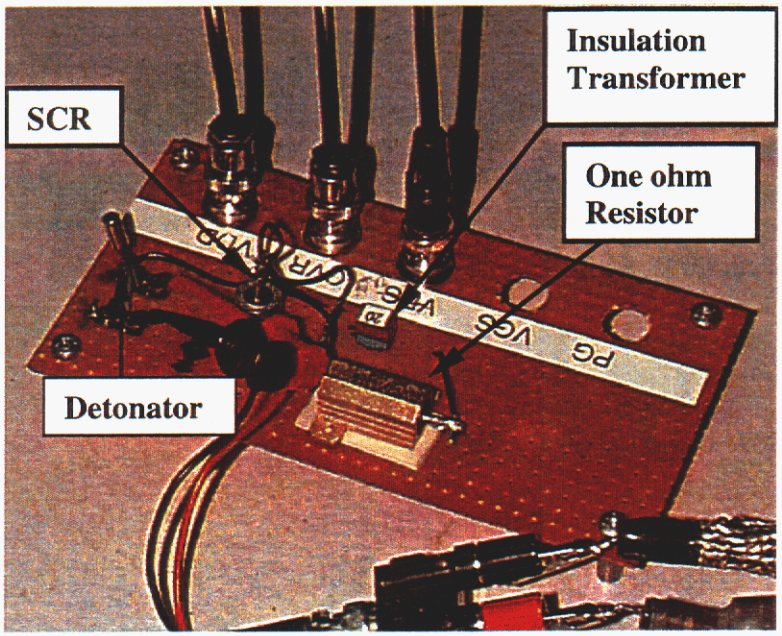

Figure 4. Gapping board.

Gapping Parameter Summary

Typical current on and voltage across a detonator for all applied current levels are shown in Figures 5 through 11. Except for the early-time inductive effect, applied current was kept approximately constant for most shots. However, as the temperature of the bridgewire increases, the increase in bridgewire resistance causes the current to drop in late times. For higher-current-level shots, this resistance loading on the source toward the end of the pulse was significant.

Several observations on these responses are in order: (1) The voltage across the EBW increased with increasing bridgewire resistance which, in turn, was caused by increasing bridgewire temperature. (2) As the bridgewire opened, the circuit inductance caused a large spike in the voltage. (3) For high current levels, the voltage did not vanish after gapping; the conductive channel remained even though the current levels were quite low. (Late-time current values for 4A and 5A DC cases are typically of tens of mA; late-time current values for high current DC cases are typically of hundreds of mA.) (4) The voltage response for 4A (Figure 5) was somewhat puzzling; it appeared that the resistance went up and then steadily went down. It was possible at a later time the bridgewire was cooling except near the center where it was eventually gapped.

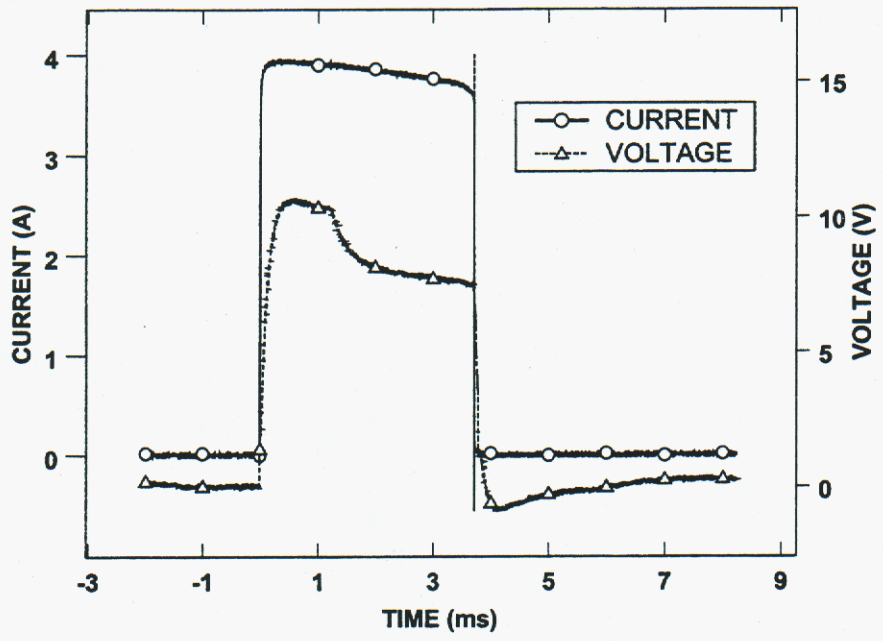

Figure 5. Current on and voltage across the EBW for a 4A shot.

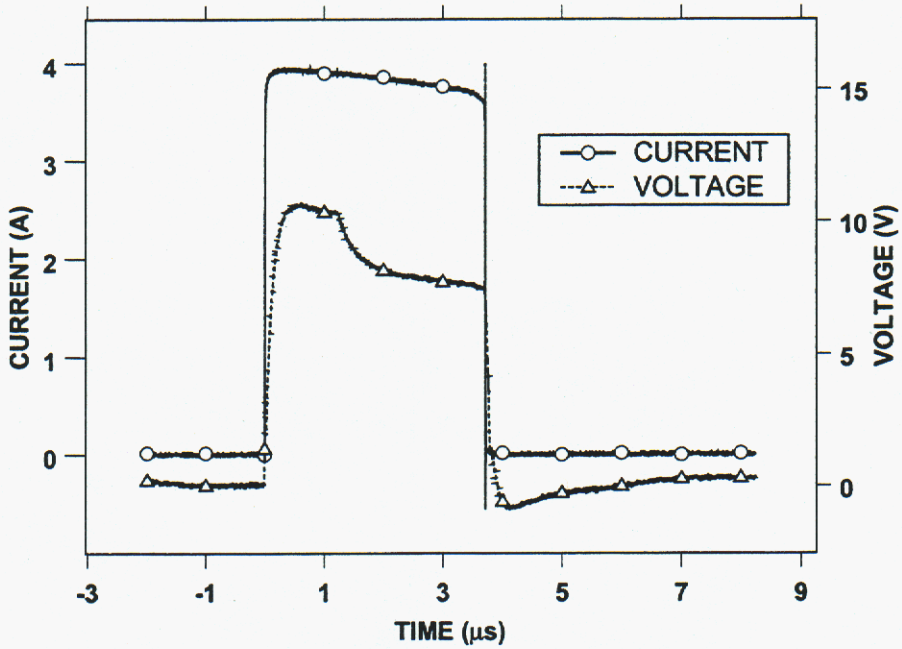

Figure 6. Current on and voltage across the EBW for a 5A shot.

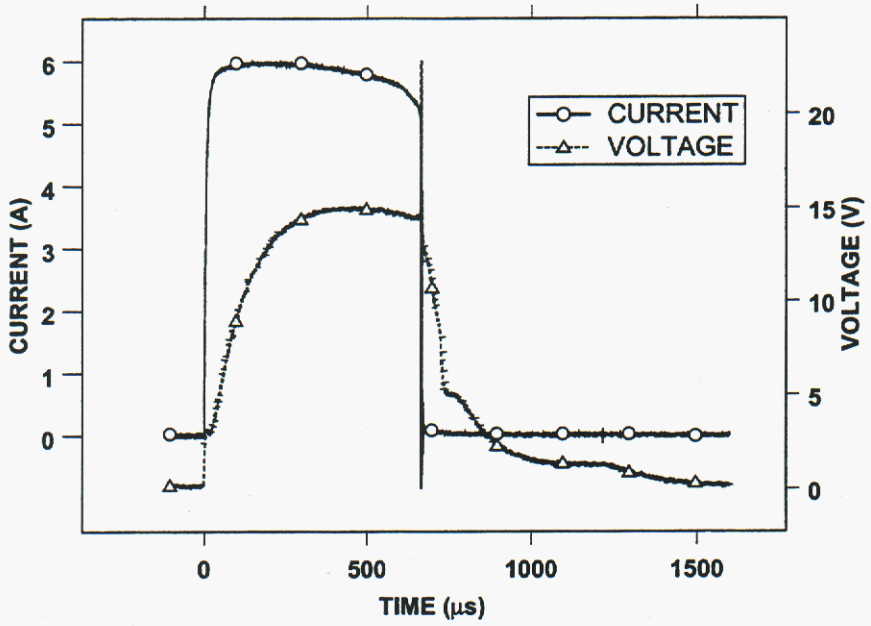

Figure 7. Current on and voltage across the EBW for a 6A shot.

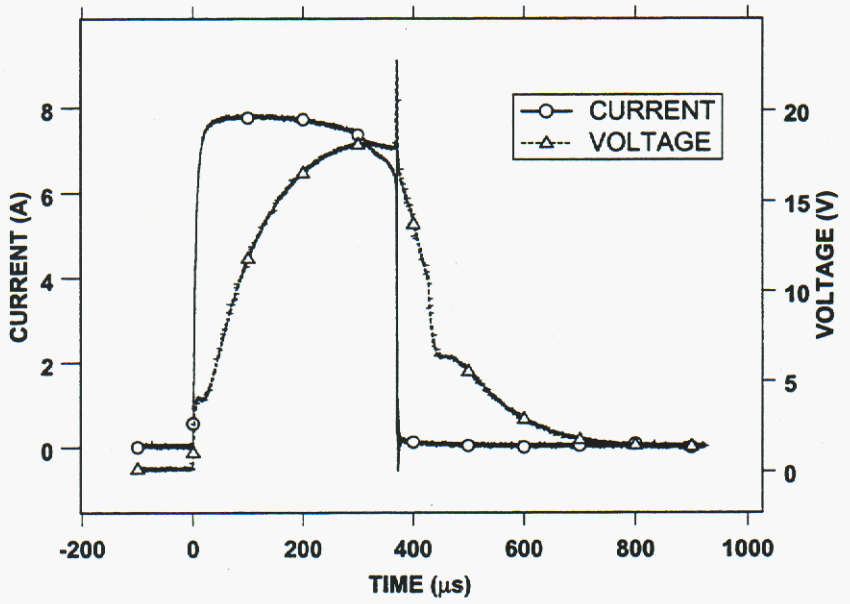

Figure 8. Current on and voltage across the EBW for an 8A shot.

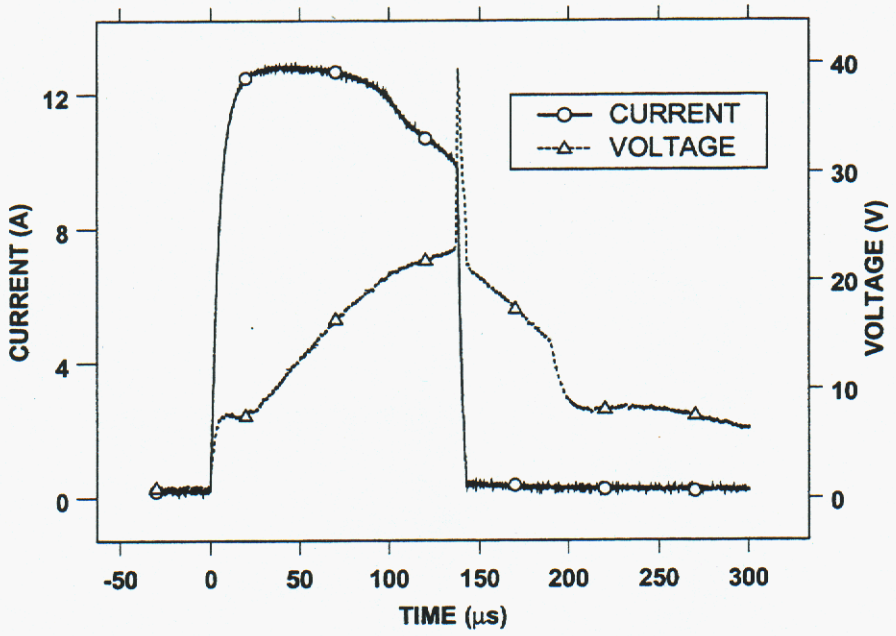

Figure 9. Current on and voltage across the EBW for a 12A shot.

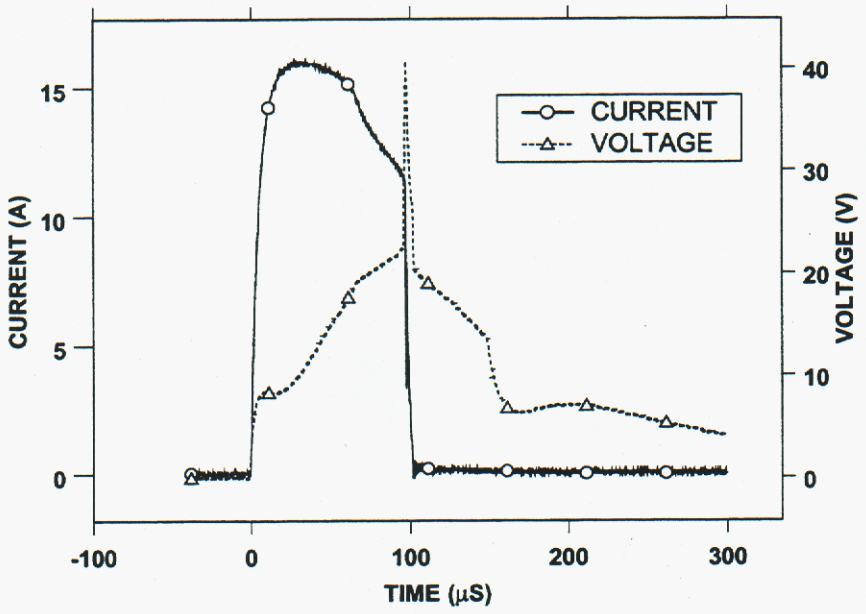

Figure 10. Current on and voltage across the EBW for a 15A shot.

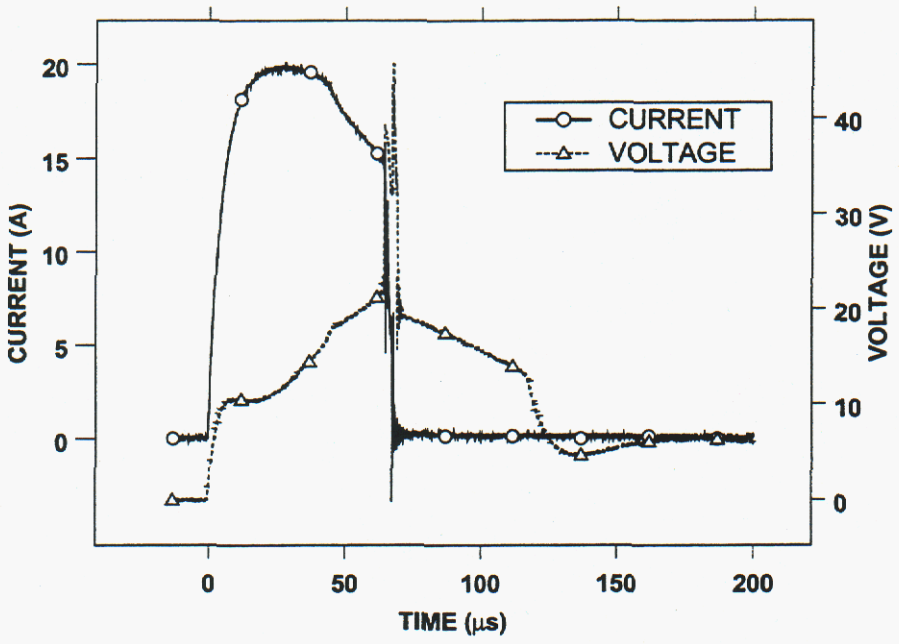

Figure 11. Current on and voltage across the EBW for a 20A shot.

Gapping parameters are summarized in Table 2 for gaps formed by a 3A current. Note the variations in time for the bridgewires to open. For three bare-bridgewire detonators, the time-to-opening ranged from milliseconds to tens of seconds; for ten full detonators, the smallest time-to-open is 18 seconds, and four bare bridgewire detonators did not open after five minutes. Full detonators took considerably more time to open because of PETN thermal loading. Gap lengths for bare detonators were measured by microscopy and gap lengths for full detonators were inferred from radiography. Gap lengths for bare bridgewire detonators formed by 3A do not differ much; the corresponding gap lengths for full detonators vary by almost a factor of two. (Three of them did not open after 5 minutes). Also, note that electrical response data for one shot was lost during the test.

3A is the threshold level for gapping; current levels lower than 3A cannot gap a 1 mil by 20 mil gold bridgewire. Other threshold data can be found in data complied by Yactor [6]. Davis also conducted some EBW gapping testing for LLNL EBWs [7].

Table 2. Gapping Parameters Gaps Formed by a 3A DC Current.

Current Level (A)	Gap Length(mils)	Time-to-opening	Detonator Type
3	4.8	14.8s	Bare
3	4.1	39.7ms	Bare
3	4.0	3.92ms	Bare
3	3.0	18s	Full
3	6.0	45s	Full
3	3.0	60s	Full
3	5.0	>100s	Full
3	2.5	210s	Full
3	3	(not available)	Full
3 (on a total of 4 units)	Not Open	After 300s	Full

Gapping parameters are summarized in Table 3 for gaps formed by other current levels. Note the difference in time-to-open between the bare bridgewire detonators and full detonators. For 4A, the full detonator took 3.8 ms for the bridgewire to open, while the bare bridgewire detonator only took 1.7 ms; for 5A, the full detonator took 1.12 ms, while the bare bridgewire detonators took 0.82 ms; for 6A, the time-to-open is 660 μs versus 560 μs, respectively; finally for 8A, the time-to-open is 360 μs versus 315 μs. The difference here is caused by PETN thermal loading; the lower the current level, the longer it takes to open the bridgewire, the greater the heat loss caused by PETN. Also, for currents greater than 12A the gap opens all the way to the post-to-post spacing of 20 mils.

Table 3. Gapping Parameters for Gaps Formed by Other Current Levels

Current Level (A)	Gap Length (mils)	Time-to-Opening (average)	Detonator Type
4	6.2	1.7ms	Bare
4	5	3.8ms	Full
5	11.5	0.82ms	Bare
5	9	1.12ms	Full
6	16	560μs	Bare
6	13	660μs	Full
8	17	315μs	Bare
8	15	360μs	Full
12	20	147μs	Full
15	20	93μs	Full
20	20	65μs	Full

Typical microscope pictures for bare bridgewire detonators are shown in Figures 12 and 13. Note the gradual increase of the gap length from 3 A of applied current to 8A of applied current.

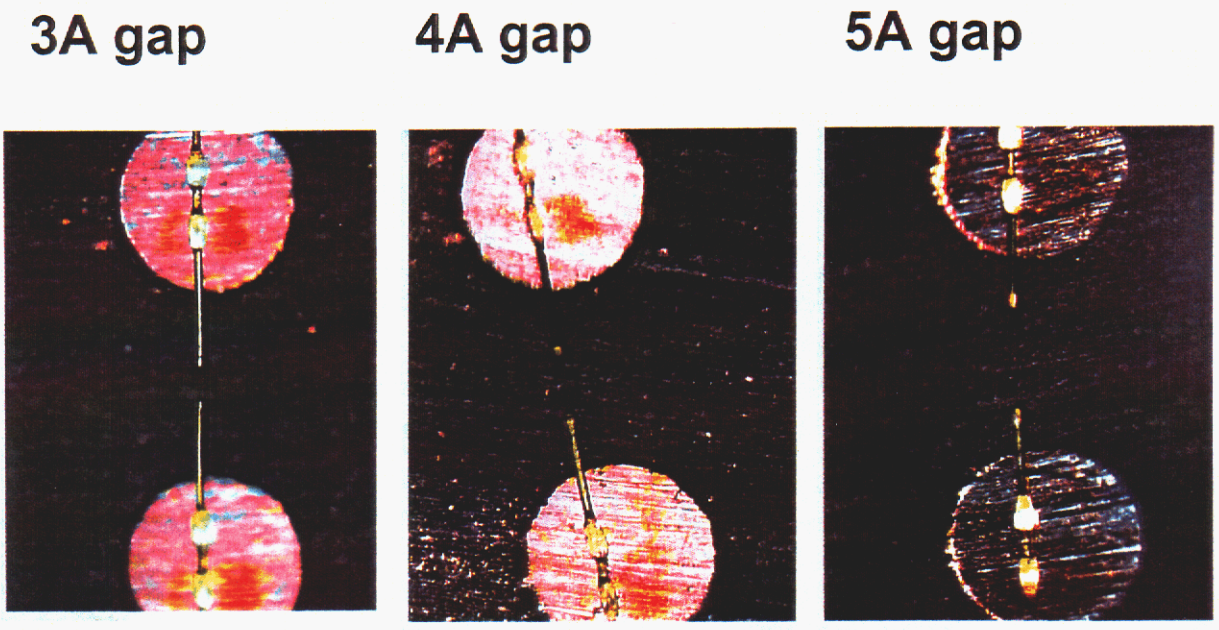

Figure 12. Microscope pictures of bare bridgewire gaps after applying 3A, 4A, and 5A, respectively.

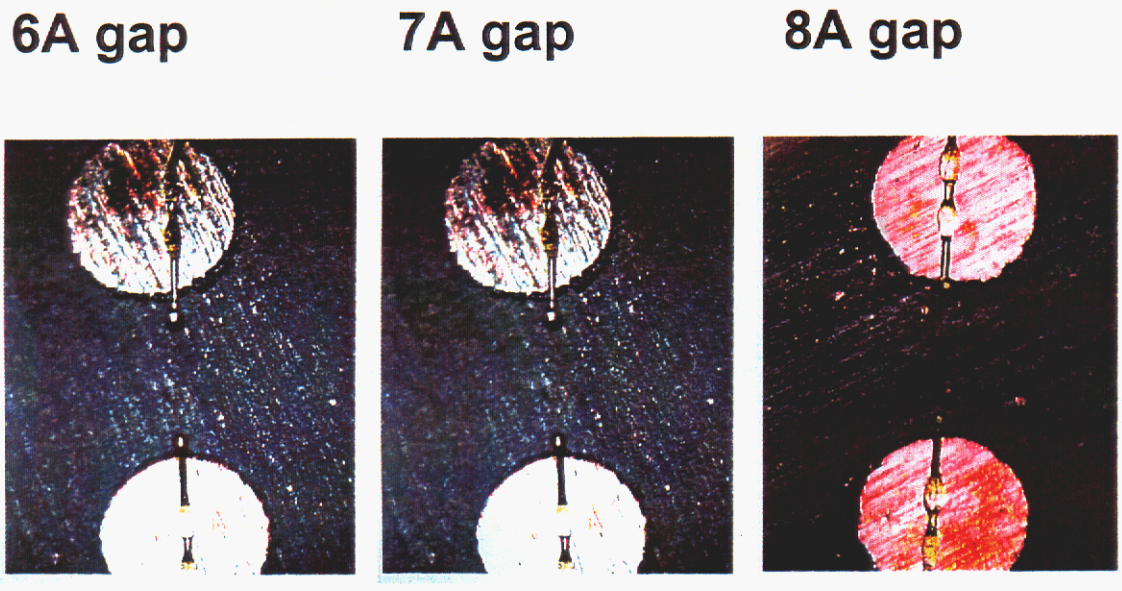

Figure 13. Microscope pictures of bare bridgewire detonators after applying 6A, 7A, and 8A, respectively.

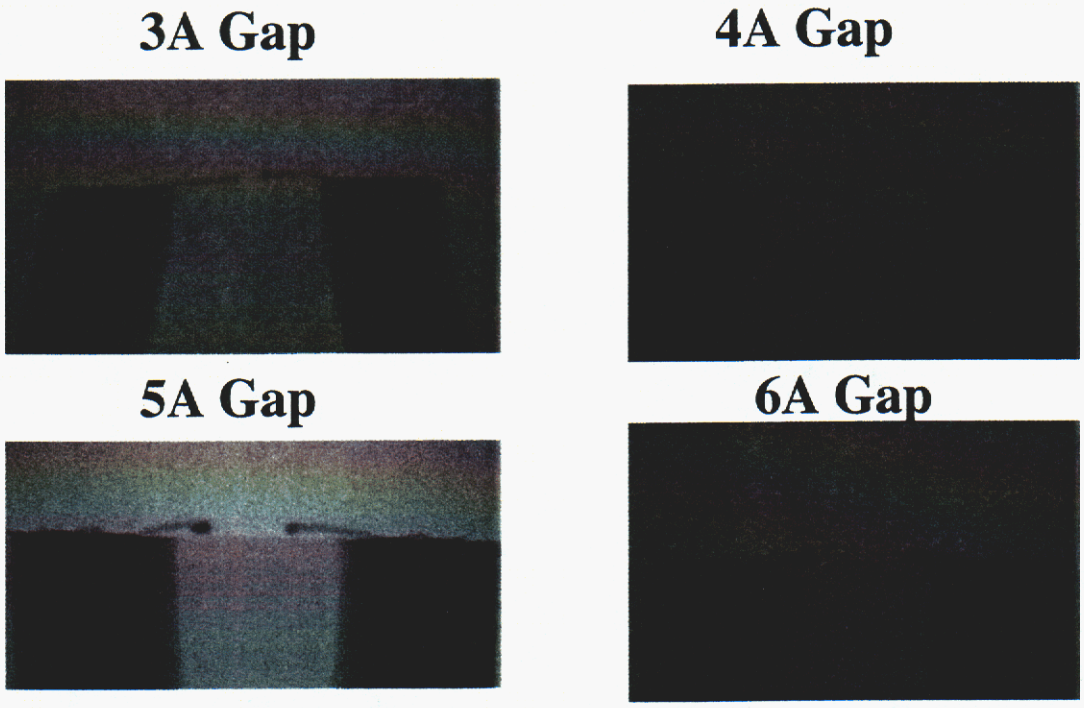

Figure 14. Radiographic pictures of gapped full detonators after applying 3A, 4A, 5A and 6A, respectively.

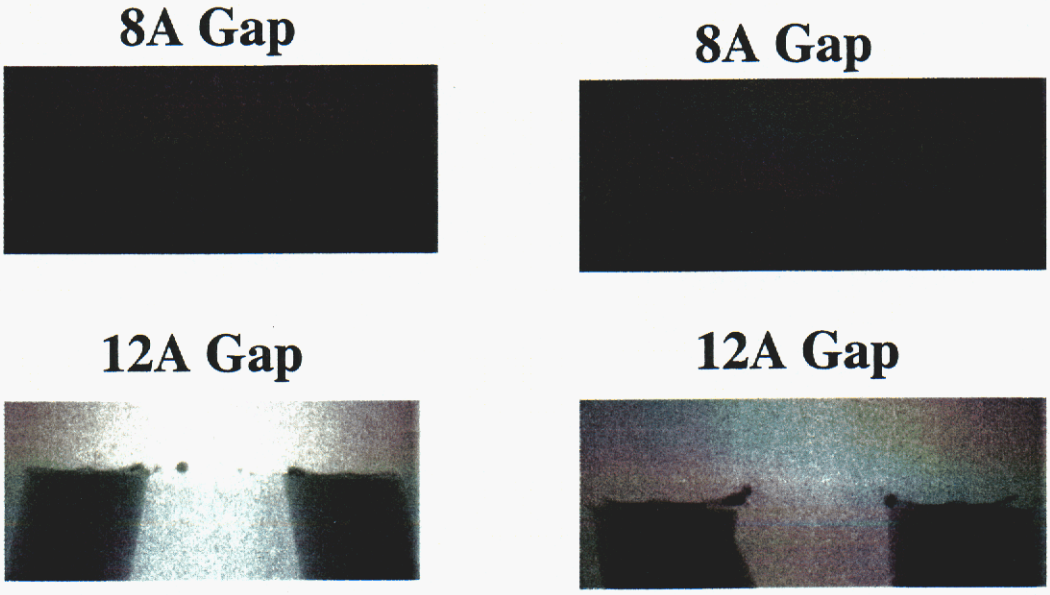

Figure 15. Radiographic pictures of gapped full detonators after applying 8A and 12A, respectively.

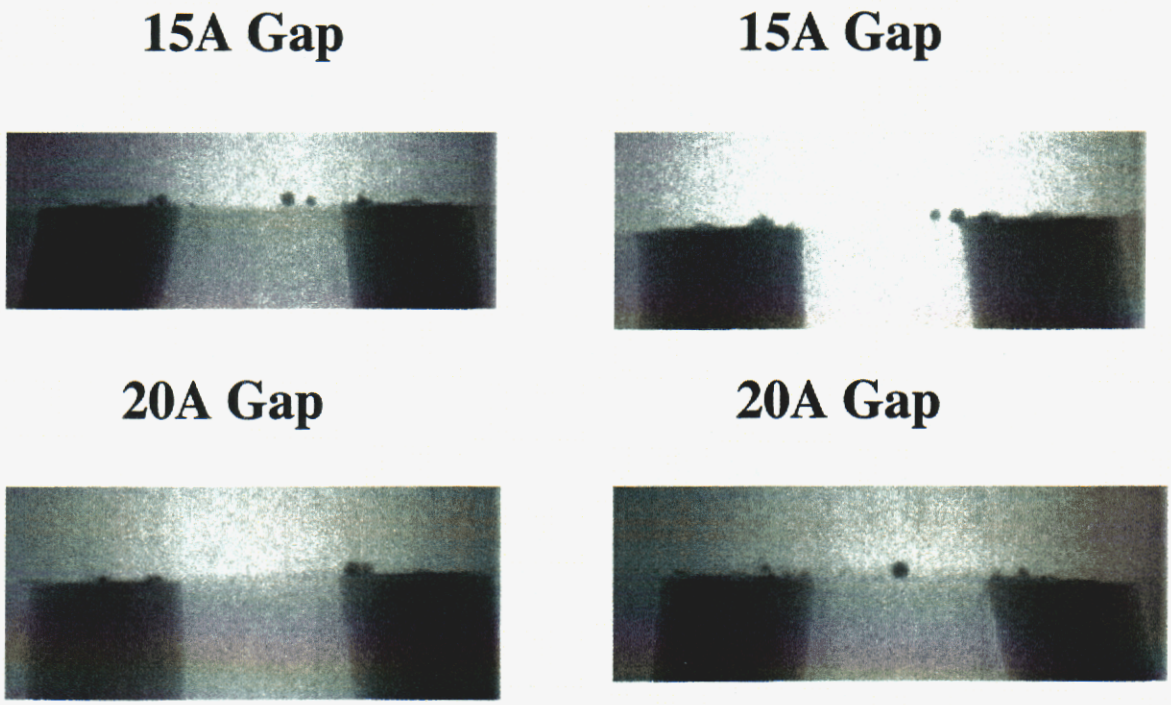

Figure 16. Radiographic pictures of gapped full detonators after applying 15A and 20A.

Radiographic pictures of full detonators are shown in Figures 14, 15, and 16. Note that the gap increased with increasing applied current. Gapping causes truncated bridgewire ends to form balls. Also, the very comlicated gap structure (formed by currents greater than 8 A) may be caused by the interaction of the vaporized gold and the surrounding PETN.

Gap length as a function of applied curent (Figure 17) indicates the negligible difference between bare bridgewire and full detonators. Also, gap length is a monotonically increasing function of applied current.

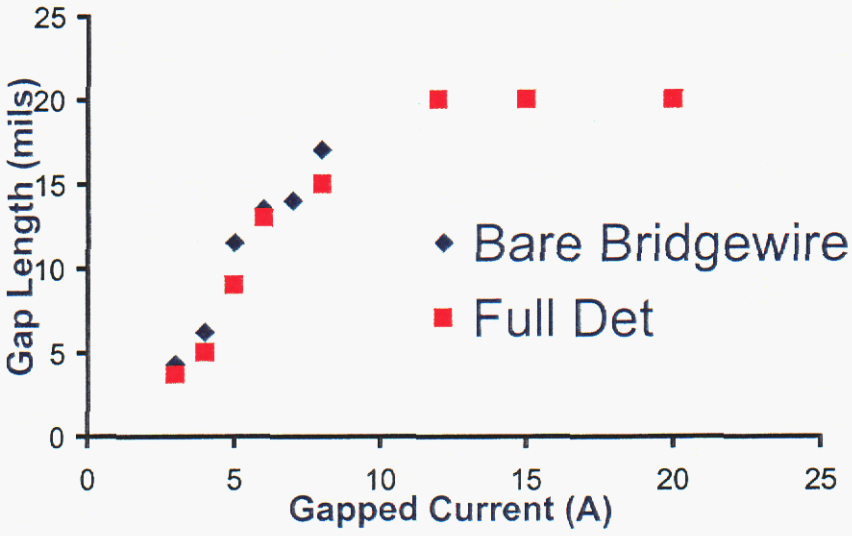

Figure 17. Gap length as a function of applied current.

Gapping Data Analysis

Action and energy for gapping EBWs are given in Figures 18 and 19. Action has a unit of A^2-sec; energy has a unit of Joule. Full detonator data (with the exception of 4A case) show a typical maximum variation of approximately 5% from the mean are shown. (The sample size is ten or eleven). The 4A data have a very large variation because they are very close to the threshold gapping value of 3A. The 3A data are not shown because some EBWs were not gapped after five minutes and also individual responses differ by many orders of magnitude. Bare bridgewire data are based on one response for each current level.

The full detonator data have consistently higher action and energy than the bare bridgewire data because of extra heat losses to the surrounding PETN.

A possible explanation for the results is in order: Typically, action required for gapping EBWs is found to be slightly less than the action required to burst the bridgewire. Energy required, on the other hand, is considerably greater than the energy required to burst the bridgewire. Gapping occurs on the order of hundreds of μs or even ms. During this time interval the liquefied metal of the wire could deform and in so doing the resistance of the liquefied column could increase. Even with the increase in energy required for gapping caused by heat losses, the required action for gapping is slightly

smaller. Another possible occurrence during gapping is that only a burst of a small portion of the bridgewire would provide enough mechanical force to cause gapping.

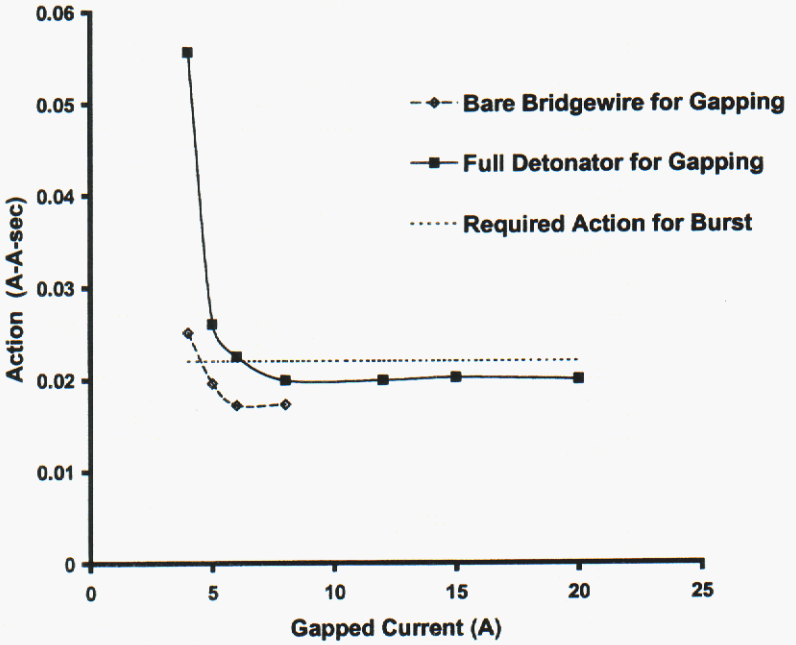

Figure 18. Required action for EBW gapping.

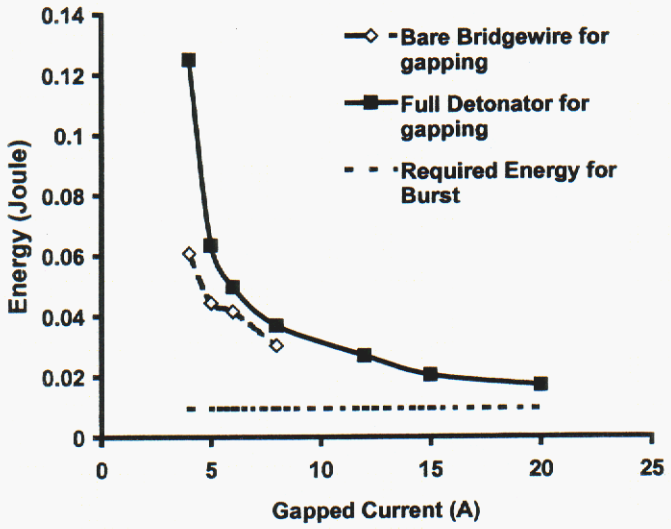

Figure 19. Required energy for EBW gapping.

It should be emphasize that because the gapping action is approximately equal to the burst action, the burst action can be used for determining the required action for gapping. Therefore, the tabulated burst action values for common metals (Table 1) can be used for predicting bridgewire gapping.

Gapping Analysis

In order to gain some insight into the gapping data, we provide an analytical theory for describing the physics of gapping. The bare bridgewire is treated here and heat loss through air is neglected. The posts are assumed to be infinite heat sinks and, for simplicity, assumed to remain at room temperature. The gold bridgewire is a very good thermal conductor and the only heat loss is thus assumed to be through the bridgewire to the posts.

The one-dimensional heat equation is

$$\frac{\partial}{\partial x}\left(k\frac{\partial T}{\partial x}\right)+g=\rho c_p\frac{\partial T}{\partial t}$$

and

$$g=\frac{I^2}{A^2\sigma},$$

where T is the temperature, k is the thermal conductivity, ρ is the density, c_p is the specific heat, σ is the electrical conductivity ($\rho_e=\frac{1}{\sigma}$ is the electrical resistivity), I is the bridgewire current and A is the bridgewire crosssection area. $\alpha=\frac{k}{\rho c_p}$ is the thermal diffusivity and, for gold, is 1.28 cm^2/sec at room temperature. g is the electrical power input per unit volume.

Note that inside the parenthesis on the left hand side of the heat equation is the gradient of temperature; the product of this gradient and the thermal conductivity is heat flow, and this whole term represents the divergence of heat flow. Therefore, the heat equation is based on energy conservation.

The temperatures at the posts are assumed to be equal and given by

$$T=T_0,\qquad x=0,\ 2L$$

where $2L$ is the distance between the posts.

Because of large temperature variation and phase transition it is more convenient to transform the dependent variable from temperature to energy. Define the local energy

density $U = \int_{T_0}^{T} \rho c_p \, dT$ and define energy deposited per volume without loss $U_d = \frac{I^2}{A^2}\int_0^t \frac{dt}{\sigma} = \frac{I^2}{A^2}\int_0^t \rho_e dt$. Assume that, initially, local energy density is given by U_i. Note that the definition of U includes heat of fusion and heat of vaporization. A heat equation with energy as a dependent variable can be written as

$$\frac{\partial}{\partial x}\left(\alpha \frac{\partial U}{\partial x}\right) + g = \frac{\partial U}{\partial t}$$

We can only solve a semi-infinite problem; therefore, we let $L \rightarrow \infty$ and treat the boundary layer near $x = 0$. The boundary condition becomes

$$U = U_0$$

Adiabatic Case

The existing data for the adiabatic case is reviewed first. Tucker et al tabulated ρ_e for gold as a function of action and ρ_e as a function of U_d. $U_d(t)$ can be obtained from $\rho_e(I^2 t)$ and $\rho_e(U_d)$. When action and energy for burst are normalized to one, a mapping from normalized action (or normalized time) and normalized energy can be obtained and is shown in Table 4.

Table 4. Energy and Resistivity as Function of Action (Normalized to Burst)

Normalized Action	Normalized Energy (U)	Resistivity (μΩ-cm)	Temperature (°C)
0	0	2.02	22
0.08	0.005	2.54	94
0.18	0.019	3.37	201
0.28	0.022	4.56	345
0.36	0.031	5.87	489
0.45	0.047	8.02	720
0.56	0.075	12.1	1063 (melt start)
0.63	0.105	26	1063 (melt end)
0.72	0.18	40	2014
0.78	0.25	49	2966 (vapor start)
0.86	0.37	65	>2966
0.94	0.49	104	>2966
0.96	0.54	120	>2966
0.98	0.6	280	>2966
0.985	0.7	420	>2966
0.99	0.78	640	>2966
0.995	0.84	840	>2966
1	1	1124	>2966 (burst)

Note that the subscript "d" for U will be dropped because Tucker et al.'s data can be used for the non-adiabatic case and U is a local state parameter. Because I is almost constant (Figures 5 through 11) and can be assumed to be constant for this analysis, action can be given by I^2t. Therefore, normalized action values can be used as time normalized to the time-to-opening.

Heat-Balance Integral

This is an approximate integral method applicable to a non-linear thermal conduction problem [8]. First, the method is applied to a semi-infinite problem, and then extended to a slab problem. Assumptions and approximations are described below:

(1) The heat conduction occurs only up to a phenomenological distance, δ (t), called the thermal layer, beyond which the local energy function is given by $U_i + U_d$, and their leading derivatives are assumed to be zero:

$$U\big|_{x=\delta} = U_i + U_d, \quad \left.\frac{\partial U}{\partial x}\right|_{x=\delta} = \left.\frac{\partial^2 U}{\partial x^2}\right|_{x=\delta} = 0$$

Although the solution of the heat equation instantaneously diffuses heat to infinity, most heat fluxes propagate with a finite velocity and the thermal layer as defined gives a very good approximation to its exact solution.

(2) Integrating the heat equation with energy as a dependent variable over the thermal layer gives the heat-balance integral:

$$\alpha\left.\frac{\partial U}{\partial x}\right|_{x=\delta} - \alpha_s\left.\frac{\partial U}{\partial x}\right|_{x=0} = \frac{\partial}{\partial t}\int_0^\delta U dx - U\big|_\delta \cdot \frac{\partial \delta}{\partial t} - \int_0^\delta g dx$$

or

$$-\alpha_s\left.\frac{\partial U}{\partial x}\right|_{x=0} = \frac{\partial}{\partial t}\left[\int_0^\delta U dx - (U_i + U_d)\delta\right] + \frac{I^2}{A^2}\int_0^\delta [\rho_e(U_d) - \rho_e(U)]dx$$

α_s is α evaluated at the post and thus assumes the value of room temperature (1.28 cm^2/sec). $\rho_e(U)$ means ρ_e as a function of U. Also, $g_d = \dfrac{\partial U_d}{\partial t}$.

(3) Assuming the resistivity as constant* along the bridgewire, we can use a third-degree polynomial for the energy profile across the thermal layer. Because of the conditions at $x = 0$ and $x = \delta$, the energy profile can be written as (Figure 20)

$$U = U_0 + \left[1 - \left(1 - \frac{x}{\delta}\right)^3\right] \cdot (U_i - U_0 + U_d)$$

---

* The resistivity is a function of temperature and thus energy deposition is not constant along the wire. However, we shall assume the resistivity as constant. Between the melt and vaporization temperature accounting for more than 90 % energy deposition, the surrounding PETN is consumed and a full-blown three-dimensional solution is required.

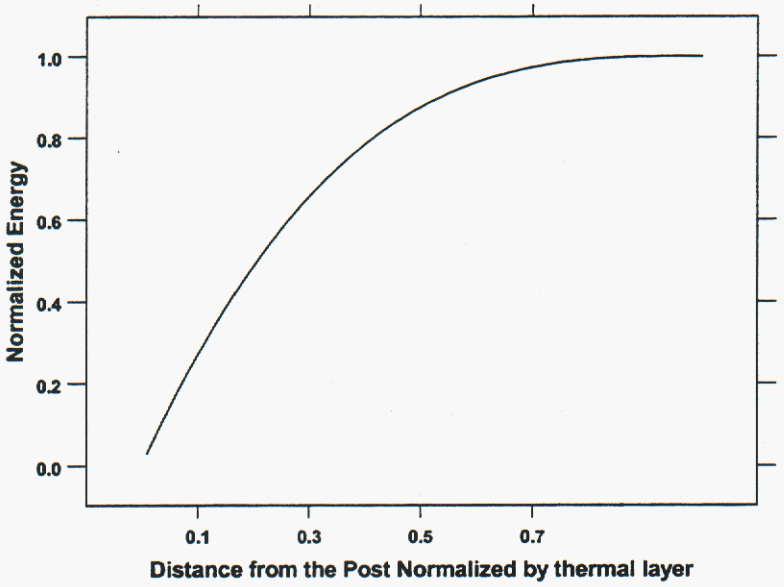

Figure 20. Normalized Energy Profile near the Post.

(4) Note that if the last term on the right hand side of the heat-balance integral is dropped (or if $\rho_e(U) = \rho_e(U_d)$), the thermal layer, δ (t), is solved by substituting the assumed energy profile into the heat-balance integral. The result is

$$\delta^2 = 24\alpha_s \frac{\int_0^t (U_i - U_0 + U_d)^2 dt}{(U_i - U_0 + U_d)^2}$$

Now the equation given for the thermal layer, δ (t), can be approximately evaluated to give

$$\delta \approx 0.21\alpha_s t_v$$

where t_v is time to bridgewire burst.

Numerical values are in order: For the $5A$ case, time-to-opening for bare bridgewire is 0.82ms; δ is evaluated as 1.48×10^{-2} cm$\approx$ 5.8 mils. Note that the microscope picture indicates the remaining bridegwire at each end as 4.25 mil (for a 11.5 mil gap). Figure 21 indicates how the thermal layer length (δ) should be compared to the remaining

bridgewire after gapping. The energy profile formula with the calculated thermal layer is consistent with the test data because some partially vaporized section would also be displaced. For the $6A$ case, time-to-opening for bare bridgewire is 560 μs; δ is evaluated as 1.22×10^{-2} cm ≈ 4.8 mils. The microscope picture indicates the remaining bridegwire at each end as 2 mil (for a 16 mil gap). For the $8A$ case, time-to-opening for bare bridgewire is 315 μs; δ is evaluated as 0.92×10^{-2} cm ≈ 3.6 mils. The microscope picture indicates the remaining bridegwire at each end as 1.5 mil (for a 17 mil gap).

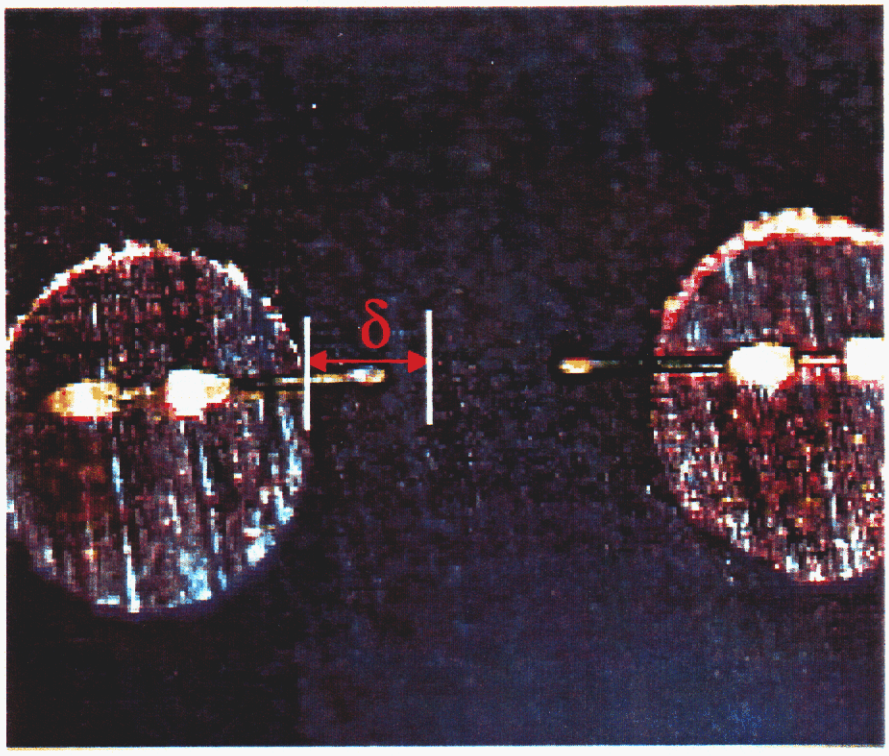

Figure 21. Comparison of the length of the remaining bridgewire (after gapping) with the thermal layer length.

Finally, we should emphasize that the approximate analysis given is very tentative and comparisons of analysis results and gap lengths are only used to indicate some underlying physics of the problem. Several limitions of the analysis are noted here: (1) Accounting for the resistivity variation along the bridgewire would make the energy profile a lot steeper than shown in Figure 20. (2) At temperatures above 3000°C, heat loss (for full detonators) in the radial direction into the PETN cannot be neglected. (3) The test data for the adiabatic case may not be reliable. In future, a computer code based on a more complete physical description of the bridgewire gapping should be used for the calculation.

Gapped EBW Sensitivity Study

Breakdown Voltage of Resulting Gapped EBWs

A capacitor short-time voltage breakdown tester, which has an upper voltage limit of 30kV, (Figure 22) was used to determine the threshold voltage of gapped EBWs. Figure 23 shows the tester's working volume, in which a gapped EBW (a test unit) was attached to the output of a high-impedance (0.5-MΩ) voltage source. The voltage across the gapped EBW under test was recorded in analog form by a one-Meg ohm strip chart recorder and in digital form by a digital panel meter. When a gapped EBW experiences a voltage breakdown, the voltage drops to zero, and the maximum output current is 5mA. In our application, a 250V/s ramp voltage was applied to a gapped EBW until the voltage dropped to zero. The highest voltage reading indicated by the strip chart or the digital panel meter was recorded.

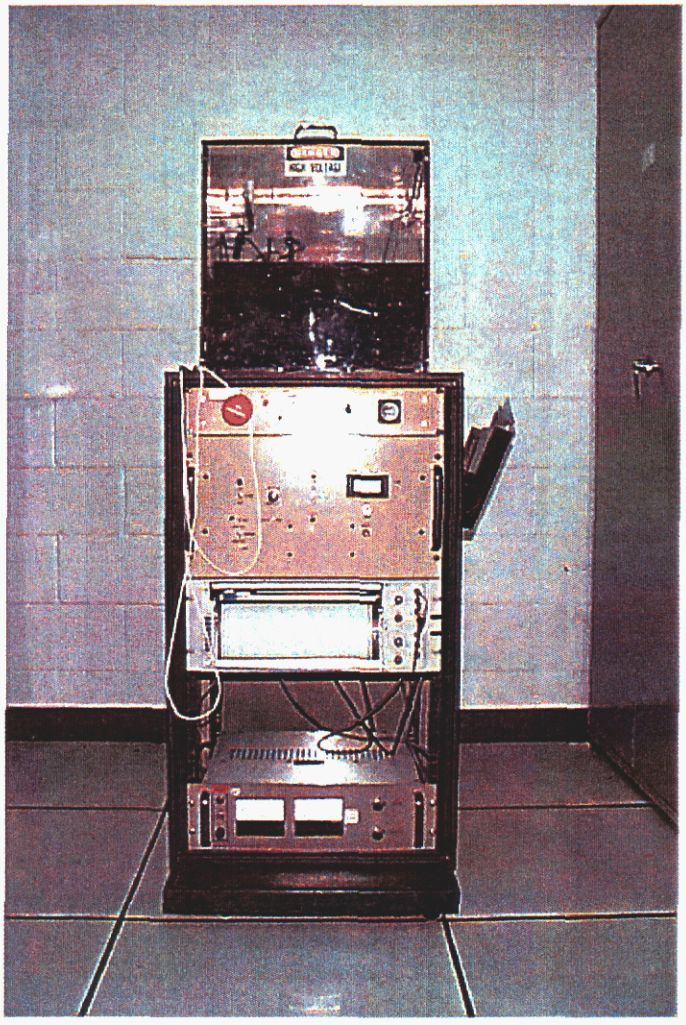

Figure 22. Capacitor short-time voltage breakdown tester.

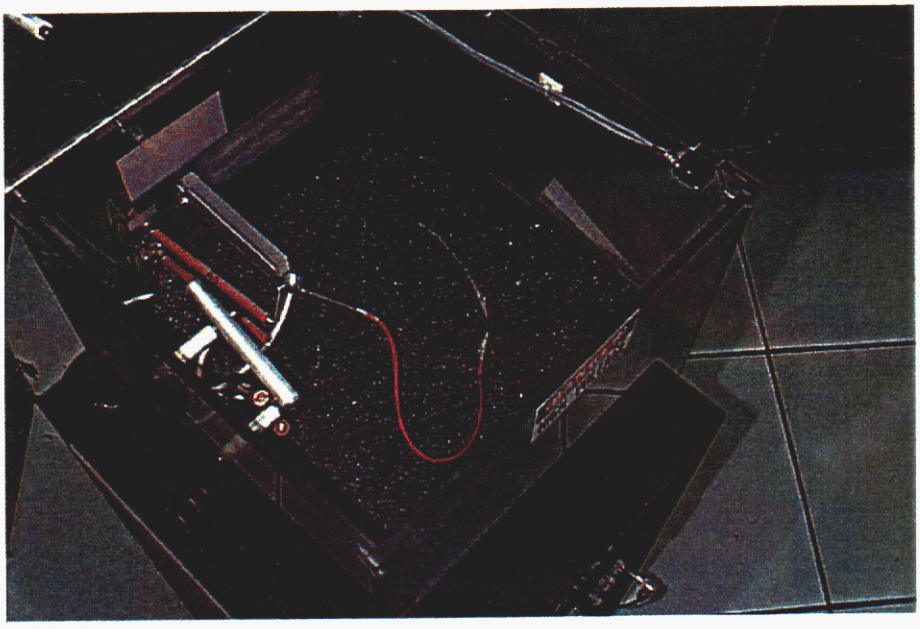

Figure 23. Working volume of a short-time voltage breakdown tester.

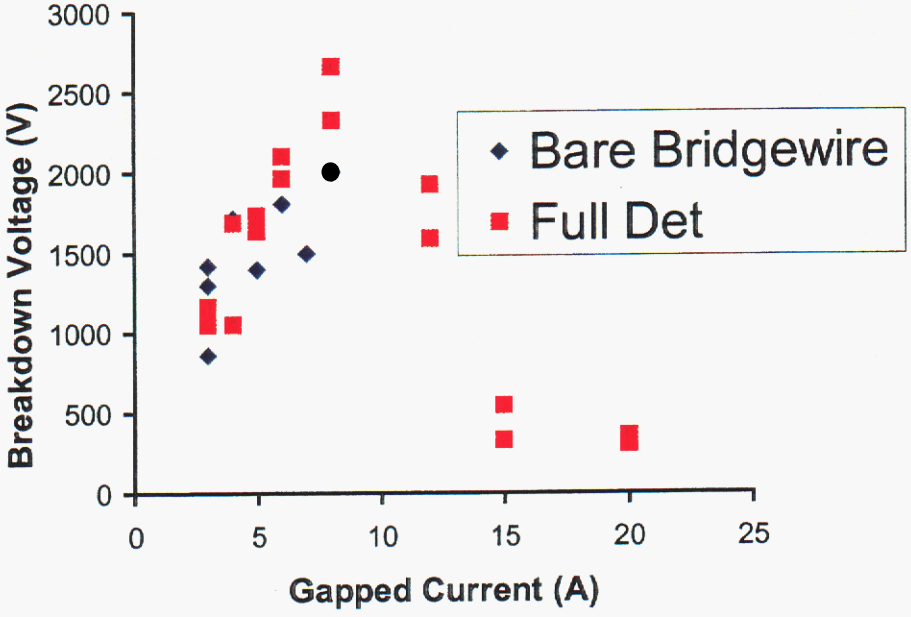

Figure 24. Breakdown voltages for different gapped current levels.

The threshold breakdown voltages for gaps formed by different current levels are shown in Figure 24 (with numerical values given in Table 5).

Table 5. Breakdown Voltages for Different Gapped Currents

Gapped Current (A)	Breakdown Voltage (V)	Detonator Type
3	860, 1290, 1410	Bare
3	1160, 1050	Full
4	1710	Bare
4	1050, 1680	Full
5	1390	Bare
5	1630, 1730	Full
6	1800	Bare
6	1960, 2100	Full
7	1490	Bare
8	2000	Bare
8	2320, 2660	Full
12	1580, 1920	Full
15	320, 540	Full
20	300, 350	Full

There is no significant difference in breakdown voltage between the bare bridgewire and full detonators. The breakdown voltage increases with increasing gap length (Figures 17 and 24) and reaches a peak at 17 mils (for a bare bridgewire) or 15 mils (for full detonators) with an 8A gapped current. For gapped currents above 12A, the gap extends all the way; however, the breakdown voltage for 12A drops somewhat from that for 8A and the breakdown voltages for 15A and 20A drop to approximately 300V. These low threshold breakdown voltages approach the Paschen curve's minimum; a carbon track on the plastic header may have reduced the actual gap length to much less than one mil.

Detonation Sensitivity of Gapped EBWs

Cable Discharge System

The Sandia Cable Discharge System (CDS) developed by the Explosive Component Facility includes an electrical energy source with six 1000-foot RG218 coaxial cables for electrical energy storage, which is charged by a high-voltage power supply (providing voltage up to 100kV). A gas pressurized, self-breaking switch, together with diagnostic, instrumentation and data acquisition systems, completes the CDS. More details on the CDS can be found in Reference 5.

Detonator Test Configuration

Figure 25 shows the output of the cable discharge system. Six, 1000-foot RG218 cables (in black) are connected in parallel at the intput to the gold pneumatic switch on top of the gray work stand. The stainless steel line exiting to the side of the switch is a nitrogen pressurized/vent line. The output of the switch matches to a 50-ohm flat cable. Current measurements were accomplished by incorporating a 5 milliohm current viewing resistor on the shield side of the cable. The EBW (with the aluminum witness block glued to the end) is attached to the flat cable and also to the leads of the voltage probe (as shown in Figure 26).

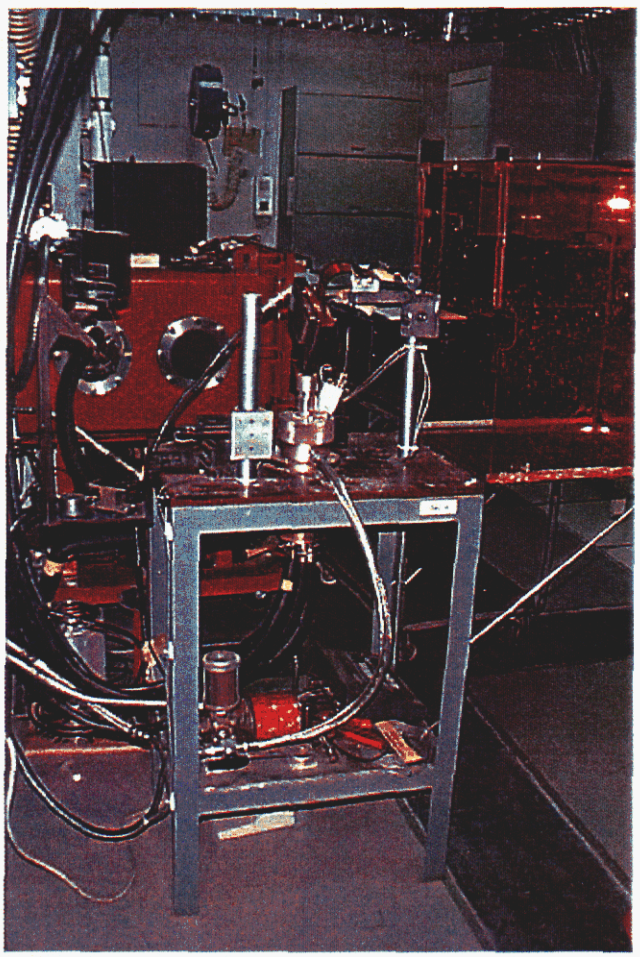

Figure 25. Working volume and output interface of the Cable Discharge System.

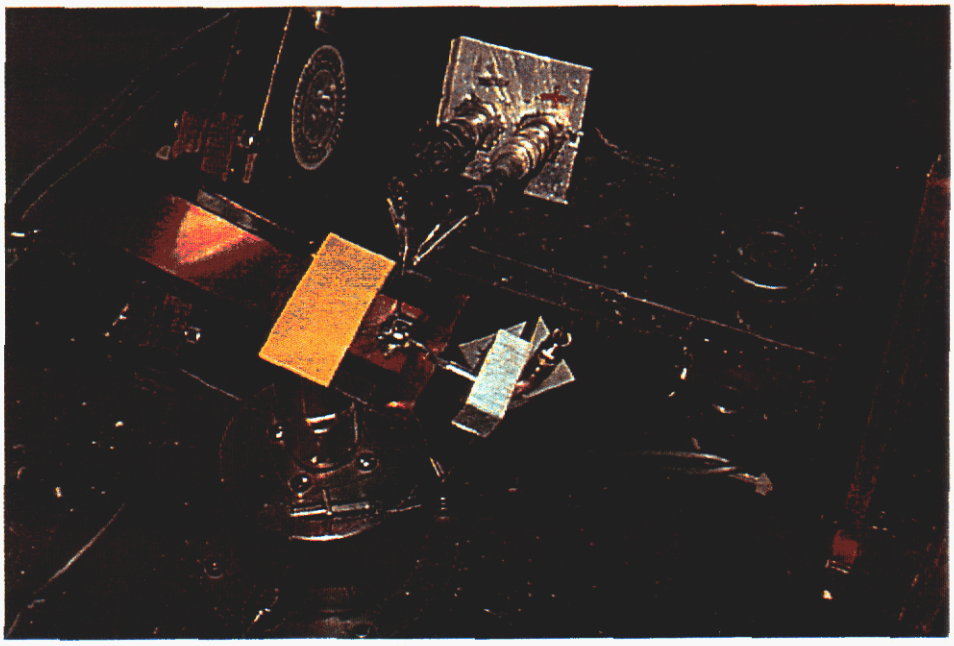

Figure 26. Detonation test configuration.

The approximate discharge-current level was first prescribed. The current level was obtained by trial shots to a short-circuit load by adjusting the power supply voltage setting. The pressure switch was then triggered to discharge the current through the EBW under test. The resulting EBW can be either deflagrated or detonated. Aluminum witness blocks can be used to distinguish between deflagration and detonation. Detonation left a dent on the block, while deflagration left only a burn mark.

A summary of shots for discharge current versus gapped current is shown in Figure 27. These shots were witnessed by aluminum blocks (Figure 28). Each scatter point in Figure 27 corresponds to each block in Figure 28. Note that the 5A gapped current has five shots with two detonations.

The detonation blocks for Figure 28 are: (1) the pristine detonator, (2) the right block for the 4A case, (3) two far right for the 5A case, (4) the right one for the 6A case, (5) the right one for the 8A case, and (6) the right one for the 12A case.

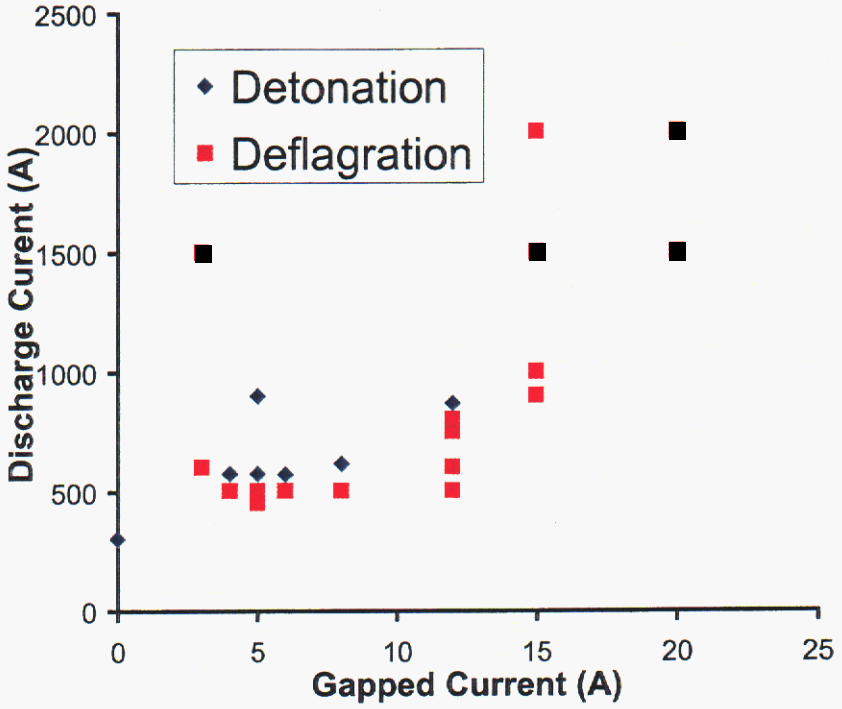

Figure 27. Detonation parameters for gapped current levels.

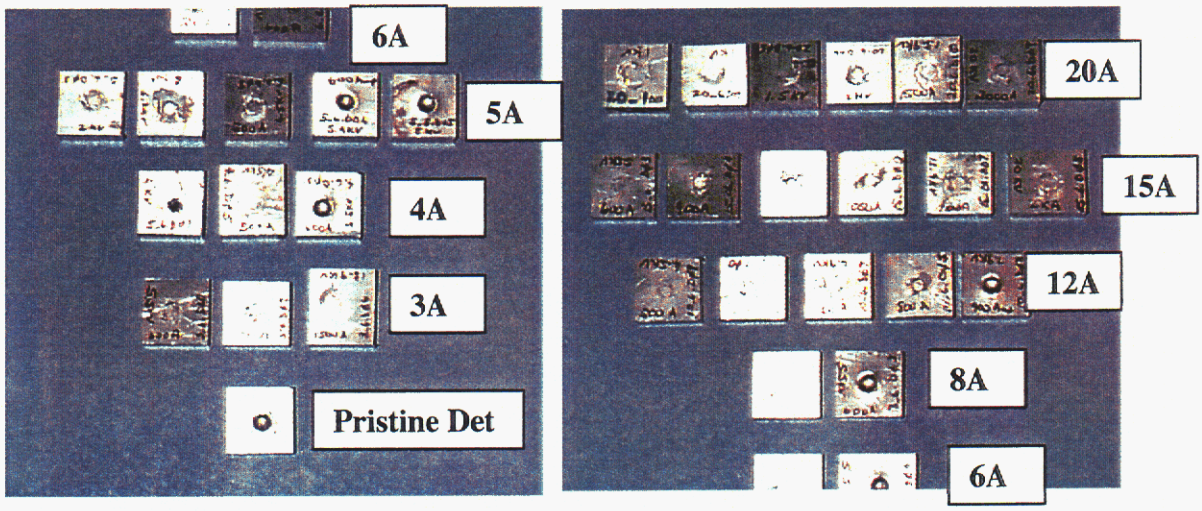

Figure 28. Aluminum witness blocks. The detonation blocks are: (1) the pristine detonator, (2) the right block for the 4A case, (3) two far right for the 5A case, (4) the right one for the 6A case, (5) the right one for the 8A case, and (6) the right one for the 12A case.

Basic deflagration current and voltage responses (Figure 29) are the transmission line discharge to a low-impedance load. The detonation responses (Figure 30) are similar, but only the first half-cycle is shown.

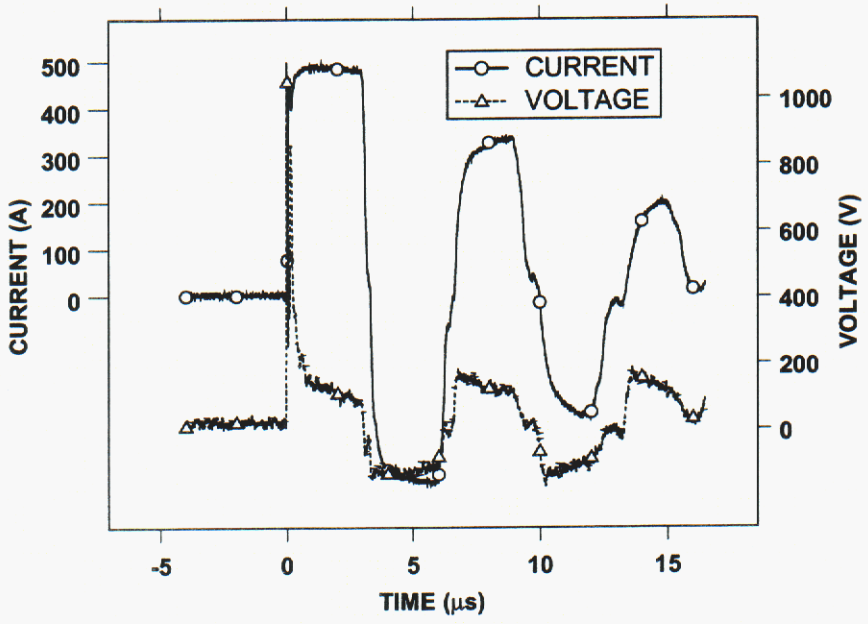

Figure 29. Typical deflagration current and voltage responses.

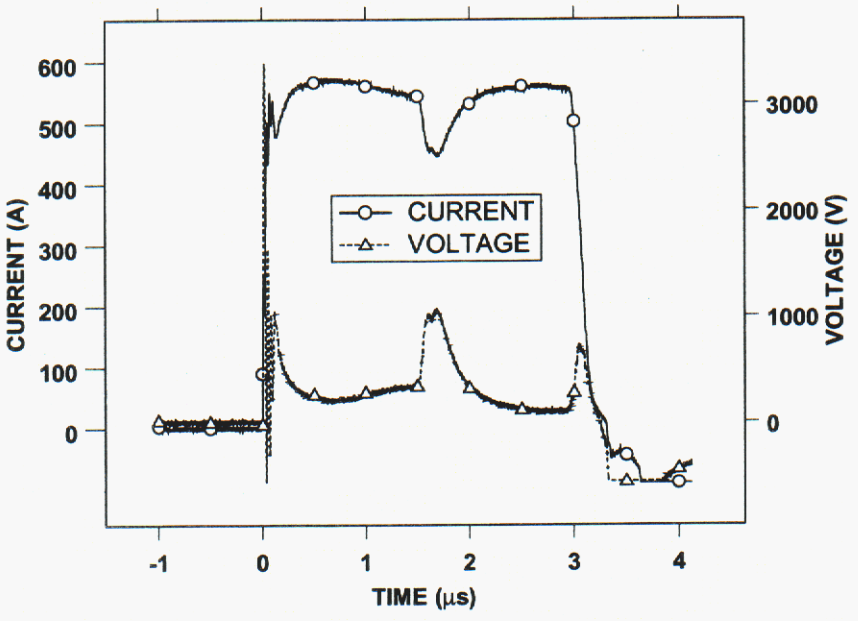

Figure 30. Typical detonation current and voltage responses.

Typical deflagration responses (Figure 29) are for an EBW gapped by a 5A current. At 160ns, the current drops to 398A, but the voltage increases to 856V (a maximum); at this instant, the remaining bridgewire burst. This is confirmed by the required burst action for the bridgewire.

In contrast, the typical detonation current response (Figure 30) has two dips: the first dip corresponds to the bursting of the remaining bridgewire and the second dip corresponds to the establishment of a hot arc leading to detonation. The time corresponding to the second dip in current is here called the detonation time. Note that voltages corresponding to these current dips are local peaks (Figure 30).

Table 6 gives a summary of detonation response characteristics (discharge current level and detonation time) for all detonation responses. Note that gapped EBWs have higher threshold detonation currents than the normal mode firing current. The readers are referred to the postmortem section, which follows immediately after this section. For large gapping currents (above 8 A), the gapping current could burn some PETN surrounding the bridgewire and the gap; therefore, it takes a lot more energy or action to detonate the PETN further away from the bridgewire location. Note that EBWs gapped by 3A (not included in Table 6) cannot be detonated because of the large energy deposition on the detonator. Also, gapped EBWs for the 15A and 20A cases can be detonated because the mechanical forces caused by the bridgewire burst probably consumed most of the surrounding PETN.

Table 6. Summary of Detonation Response Characteristics

Current Level (A)	Gap Length (mils)	Discharge Current	Detonation Time
0 (pristine)	0	300	290ns
4	6	573	1.69μs
5	8	900	1.4μs
5	8.5	570	1.7μs
6	14	570	1.71μs
8	15	615	1.68μs
12	20	868	1.8μs

Postmortem of Gapped EBWs

Two gapped full detonators for each gapped current level (3A, 4A, 5A, 6A, 8A, 12A, 15A, and 20A) were cut at the bridgewire and initial pressing interface. The exact location of the interface may be off by a few thousandths of an inch or even less.

The left figure of Figure 31 shows the bridgewire and header for the 3A gapped EBW; the corresponding right figure indicates the PETN powder and the detonator case. The center of the cup the PETN color turned yellow presumably caused by long exposure to a 3A current deposition of a large amount of energy; as a result, the PETN surface near the gap and the remaining bridgewire became non-granular and the 3A-gapped EBW cannot be detonated.

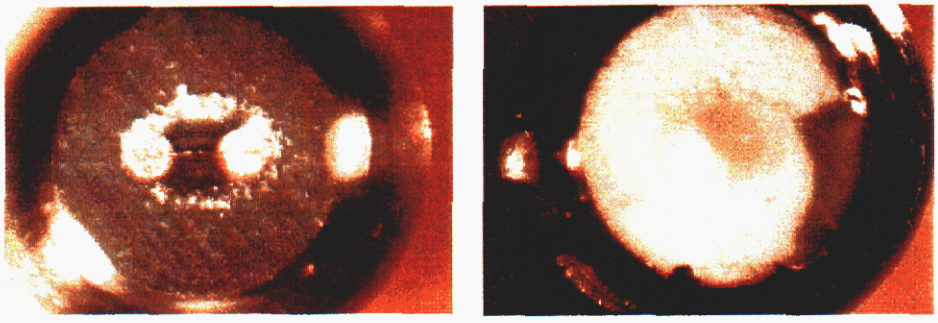

Figure 31. Cross-sectional views (the left is for the bridgewire and header, and the right for the PETN powder) for a 3A-gapped EBW.

The resulting gapped EBWs gapped by 4A, 5A, 6A and 8A were opened at the header interface and shown in Figures 32 through 35. Note that the 4A to 6A gaps were surrounded by presumably the melted and solidified PETN with a small burn cavity inside the PETN cocoon. The cocoon for the 8A gap broke near the center of the gap and the burn cavity start to show. However, the PETN powders can be seen between the posts. These gapped EBWs have been detonated by approximately 600A.

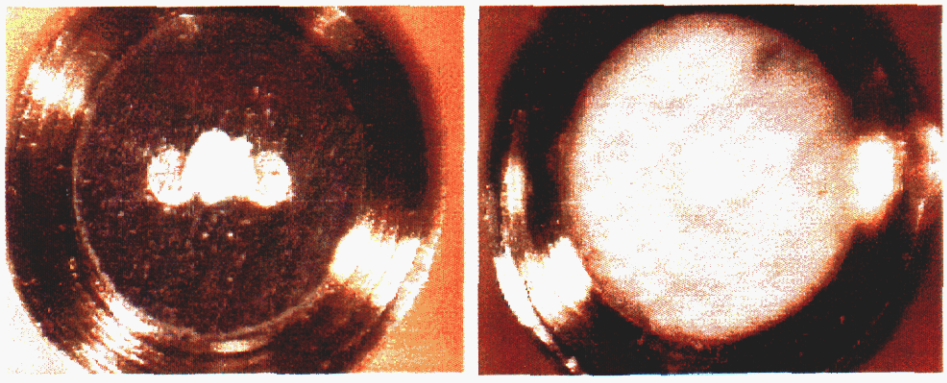

Figure 32. Cross-sectional views (the left is for the bridgewire and header, and the right for the PETN powder) for a 4A-gapped EBW.

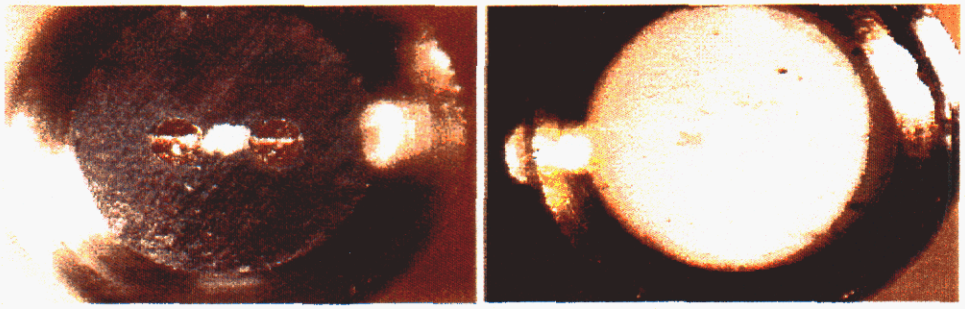

Figure 33. Cross-sectional views (the left is for the bridgewire and header, and the right for the PETN powder) for a 5A-gapped EBW.

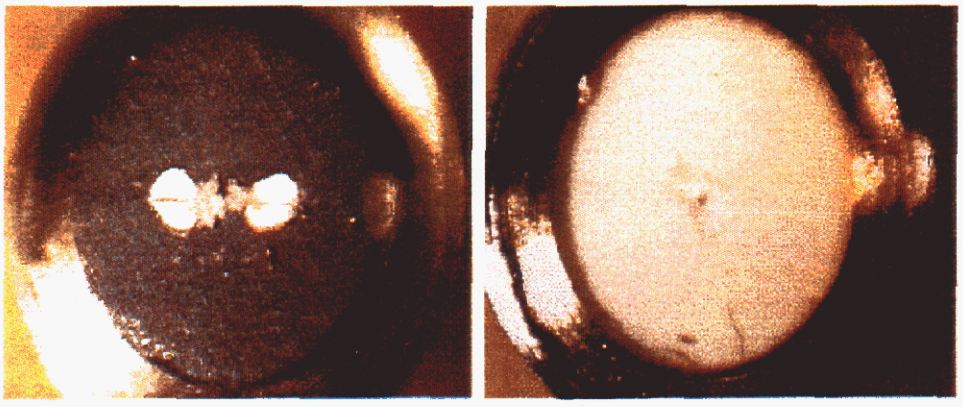

Figure 34. Cross-sectional views (the left is for the bridgewire and header, and the right for the PETN powder) for a 6A-gapped EBW.

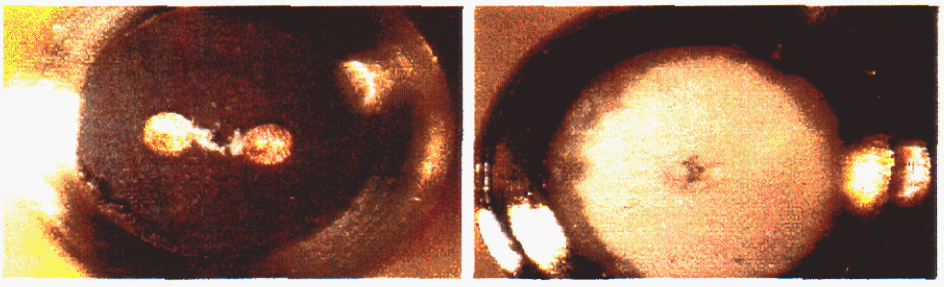

Figure 35.. Cross-sectional views (the left is for the bridgewire and header, and the right for the PETN powder) for an 8A-gapped EBW.

Figure 36 shows a 12A-gapped EBW with a burn cavity with a bridgewire length in all three dimensions. However, it is interesting to note that a current of 868A detonated one of these 12A-gapped EBWs.

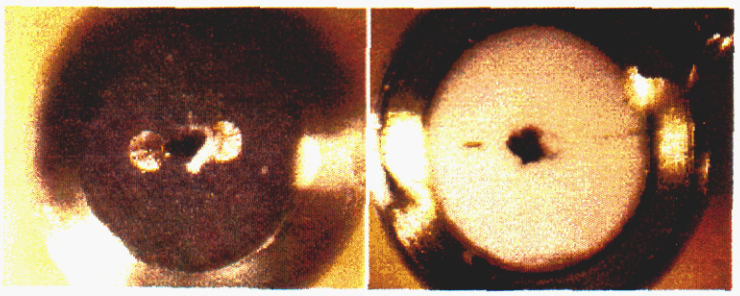

Figure 36. Cross-sectional views (the left is for the bridgewire and header, and the right for the PETN powder) for a 12A-gapped EBW.

Finally, the large burn cavities on the 15A-and 20A-gapped EBWs (Figures 37 and 38) prevented detonation from occurring even after applying a 2000A current.

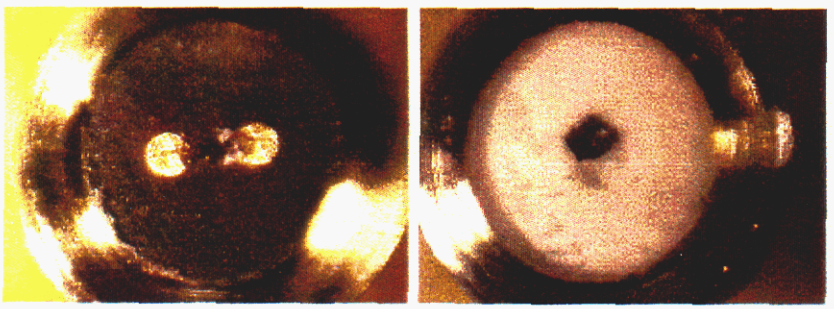

Figure 37. Cross-sectional views (the left is for the bridgewire and header, and the right for the PETN powder) for a 15A-gapped EBW.

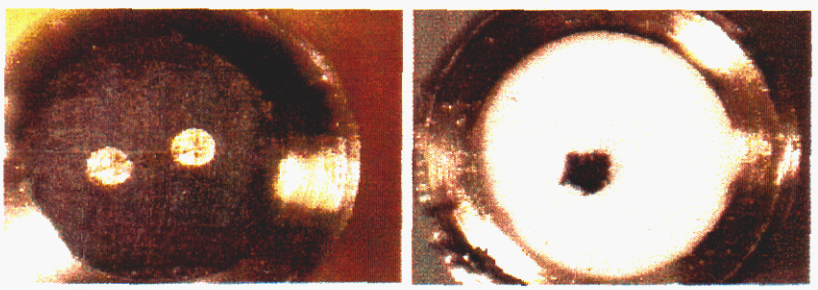

Figure 38. Cross-sectional views (the left is for the bridgewire and header, and the right for the PETN powder) for a 20A-gapped EBW.

Conclusions

Ten bare bridgewire detonators and one hundred full detonators (commercial EBW: RP-87) were gapped by DC currents of different levels and the resulting gapped EBWs were subjected to voltage breakdown and detonation characterizations.

EBW Gapping

Current levels of 3A, 4A, 5A, 6A, 7A and 8A were used to gap bare bridgewire detonators and the gaps were captured by a microscope. Current levels of 3A, 4A, 5A, 6A, 8A, 12A, 15A, and 20A were used to gap full detonators and the gaps were radiographed.

Because current is kept constant, the voltage response increases with increasing bridgewire resistance, which, in turn, is caused by increasing bridgewire temperature. Also, as the bridgewire opens, the circuit inductance causes a large spike in voltage. Gap length is found to be a monotonic function of gapped-current level. The heat equation is solved approximately to explain the trend in test data. The required action for EBW gapping is found to be approximately given by the burst action for the bridgewire, although the required energy for gapping is considerably higher than the burst energy for the bridgewire. This emperical data on action can be used to predict the occurrence of bridgewire gapping.

Sensitivity of Gapped EBWs

The resulting gapped EBWs are used to determine their voltage breakdown threshold levels and detonation characterization. The breakdown voltage threshold is not a monotonic function of gap length. The breakdown voltage has a peak with a 15-mil or a 17-mil gap formed by 8A. The breakdown voltages for the gap extended between the posts (20 mils) formed by 15A or 20A are approaching the Paschen minimum of 300V. A carbon track on the plastic header may be a possible explanation for this, having reduced the actual gap length to considerably less than one mil.

Finally, gapped EBWs have higher threshold detonation currents by at least a factor of two as indicated by data than the normal mode firing current. Postmortem indicated that the gapping current has burned most PETN surrounding the bridgewire and the gap. Therefore, it takes a lot more energy or action to detonate the remaining PETN, which is further away from the bridgewire. This explains why no detonation occurred for gapped EBWs formed by 3A, 15A, and 20A. Gapped EBWs formed by 3A could not be detonated because the large energy deposition on the detonator has transformed the phase of PETN. Also, gapped EBWs formed by 15A and 20A could not be detonated because the burned PETN cavities were too large for the burst mechanical force to reach.

Safety Implications

It is possible that an electrically gapped EBW can be subjected to mechanical vibrations and possibly move the pristine PETN to contact the bridgewire. Some tests have been

conducted to address this issue. However, current data indicated that gapped EBWs become even less sensitive after being exposed to the STS mechanical vibration spectrum.

However, because it is impossible to foresee conditions, which could make the gapped EBW more sensitive, it is prudent to assume that, for safety considerations, gapped EBWs are as sensitive as spark gap EBWs.

References

[1] Tucker, T. J., J. E. Kennedy, and D. L. Allensworth, "Secondary Explosive Spark Detonators," the Proceedings of the 7th Symposium on Explosives and Pyrotechnics, the Franklin Institute Research Laboratories, September 8-9, 1971.

[2] Furnberg, C. M., "Bridgewire Burnout Investigation for the XW-63," SCL-TM-65-16, February 1966.

[3] Tucker, T. J. and R. P. Toth, "EBW1: A Computer Code for the Prediction of the Behavior of Electrical Circuits Containing Exploding Wire Elements," SAND75-0041, April 1975.

[4] Chen, K. C., and W. P. Brigham, "Perliminary Gapping Test Results," presented at the Joint Firing System Conference, October 20-22, 1998.

[5] Furnberg, C. M., M. F. Deveney, E. K. Manzanares, W. P. Brigham, and G. R. Peevy, "Modeling the Resistance Behavior of High Energy Detonators," SAND98-8211, December 1997.

[6] Yactor, Richard, "Collected Development Progress Reports for LANL detonators: 1E31, 1E33, 1E34, 1E36, 1E38 and 3E1 (Draft)," February 1998.

[7] Davis, R. W., "Tools for Safety: Electrical Transients and Ohmic Heating," presented at the Joint Firing System Conference, October 12-14, 1999.

[8] Ozisik, M. N., Boundary Value Problems of Heat Conduction, New York: Dover Inc., 1968.

Distribution

2 University of California
Lawrence Livermore National Laboratory
Attn: R. S. Lee, L-281
Attn: R. W. Davis, L-125

2 University of California
Los Alamos National Laboratory
Attn: Richard Yactor
Attn: Jim Kennedy

1	MS1452	J. A. Merson, 2552
1	MS1453	G. Scharrer, 2553
1	MS1454	L. L. Bonzon, 2554
10	MS1454	W. P. Brigham, 2554
1	MS9202	R. L. Birbaum, 8418
1	MS0428	V. J. Johnson, 12301
1	MS0492	D. R. Olson, 12332
1	MS0492	M. A. Dvorack, 12332
10	MS0492	K. C. Chen, 12332
1	MS0405	T. R. Jones, 12333
1	MS0405	M. K. Fluentes, 12333
1	MS0405	Y. T. Lin, 12333
1	MS1152	M. L. Kiefer, 1642
1	MS1152	R. E. Jorgenson, 1642
1	MS1152	K. O. Merewether, 1642
1	MS1152	L. K. Warne, 1642